

An experimental study of rill sediment delivery in purple soil, using the volume-replacement method

Yuhan Huang, Xiaoyan Chen, Yu Zhao, Linqiao Ding, Banglin Luo

Experimental studies provide a basis for understanding the mechanisms of rill erosion and can provide estimates for parameter values for simulated models of the erosion process. In this study, we investigated sediment delivery during rill erosion in purple soil. We used the volume-replacement method to measure the volume of eroded soil and hence estimate the mass of eroded soil. A 12 m artificial rill was divided into the following sections: 0–0.5 m, 0.5–1 m, 1–2 m, 2–3 m, 3–4 m, 4–5 m, 5–6 m, 6–7 m, 7–8 m, 8–10 m, and 10–12 m. Erosion trials were conducted with three flow rates (2 L/min, 4 L/min, and 8 L/min) and five slope gradients (5°, 10°, 15°, 20°, and 25°). The eroded rill sections were refilled with water to measure the eroded volume in each section and subsequently calculate the eroded sediment mass. The cumulative sediment mass was used to compute the sediment concentration along the length of the rill. The results show that purple soil sediment concentration increases with rill length before eventually reaching a maximal value. That is, the rate of increase in sediment concentration is greatest at the rill inlet and then gradually slows. Steeper slopes and higher flow rates result in sediment concentration increasing more rapidly along the rill length and the maximum sediment concentration being reached at an earlier location in the rill. Slope gradient and flow rate both result in an increase in maximal sediment concentration and accumulated eroded amount. However, slope gradient has a greater influence on rill erosion than flow rate. The results and experimental method in this study may provide a reference for future rill-erosion experiments.

An Experimental Study of Rill Sediment Delivery in Purple Soil

Huang Yuhan^a, Chen Xiaoyan^{a, *}, Zhao Yu^a, Ding Linqiao^a, Luo Banglin^a


^aCollege of Resources and Environment, Southwest University/Key Laboratory of Eco-environments in Three Gorges Region (Ministry of Education), Southwest University, Chongqing, 400716, China

*Corresponding author at: College of Resources and Environment/Key Laboratory of Eco-environment in Three Gorges Region (Ministry of Education), Southwest University, Chongqing, 400716, China.

Abstract: Experimental studies provide a basis for understanding the mechanisms of rill erosion and can provide estimates for parameter values for simulated models of the erosion process. In this study, we investigated sediment delivery during rill erosion in purple soil. We used the volume-replacement method to measure the volume of eroded soil and hence estimate the mass of eroded soil. A 12 m artificial rill was divided into the following sections: 0–0.5 m, 0.5–1 m, 1–2 m, 2–3 m, 3–4 m, 4–5 m, 5–6 m, 6–7 m, 7–8 m, 8–10 m, and 10–12 m. Erosion trials were conducted with three flow rates (2 L/min, 4 L/min, and 8 L/min) and five slope gradients (5°, 10°, 15°, 20°, and 25°). The eroded rill sections were refilled with water to measure the eroded volume in each section and subsequently calculate the eroded sediment mass. The cumulative sediment mass was used to compute the sediment concentration along the length of the rill. The results show that purple soil sediment concentration increases with rill length before eventually reaching a maximal value. That is, the rate of increase in sediment concentration is greatest at the rill inlet and then gradually slows. Steeper slopes and higher flow rates result in sediment concentration increasing more rapidly along the rill length and the maximum sediment concentration being reached at an earlier location in the rill. Slope gradient and flow rate both result in an increase in maximal sediment concentration and accumulated eroded amount. However, slope gradient has a greater influence on rill erosion than flow rate. The results and experimental method in this study may provide a reference for future rill-erosion experiments.

Key words: Purple soil, Rill erosion, Sediment concentration, Flume experiment, Volume-replacement method, Ecology

30 1. Introduction

31 Rill erosion contributes significantly to water and soil loss on sloping farmland (Li et al.,
32 2008; Bhattarai et al., 2007). In regions with purple soil, rill erosion is an important mechanism
33 of erosion on hillslopes, and is the main source of sediment particles in the watershed. Rill
34 erosion therefore has a potentially important effect on the development and evolution
35 of drainage-area landforms (Cai et al., 2004; Nearing et  1997). In recent decades, many
36 different research techniques have been used to study rill erosion, as outlined
37 below. However, research into rill erosion in regions with purple soil remains limited.

38 In 1947, Ellison (1947) proposed a conceptual linear feedback model to describe the
39 influence of rill sediment concentration on soil erosion process. In 1982, Foster et al. (1982)
40 distinguished rill erosion from interrill erosion and found that rill erosion led to an increase in
41 eroded sediment particles compared with interrill erosion. Abrahams et al. (1992) subsequently
42 conducted a more detailed and comprehensive study on the mechanisms of rill erosion and the
43 contributing factors. Since then, an increasing number of researchers in China and elsewhere
44 have begun to research rill formation, the characteristics of rill flow hydraulics, and the process
45 of rill erosion.

46 In 2002, Zhang et al. designed a series of laboratory experiments to simulate rill erosion
47 and conducted an energetic analysis of the effect of dynamic conditions and rill length on the
48 degree of erosion. Xiao et al. (2003) used double flumes (a sand flume and an experimental
49 flume) in runoff plots on an upper slope on the Loess Plateau to study the impact of flow rate and
50 slope gradient on erosion yields in the plateau region. Yuan et al. (2010) studied rill runoff and
51 sediment transport on loess slopes with constant-flow artificial drainage combined with rainfall
52 simulation. Zhao et al. (2014) also studied rill runoff and sediment transport on loess slopes but
53 used laboratory experiments that simulated runoff scouring to infer a computational formula for
54 runoff and sediment-transport rate.

55 Casali et al. (2006) advanced a volumetric method that estimates rill volume, and hence
56 erosion, from a series of cross-sectional areas along the eroded rill, on the assumption that the

57 eroded rill volume is equal to the volume of eroded soil. They highlighted that changes in rill
58 size and morphology can introduce measurement errors with this method. An alternative method
59 for measuring rill volume is to refill the rill with soil, tiny foam particles, rice grains, or other
60 such materials (Zheng, 1989). However, in these previous studies, the rills were not well defined;
61 rills of various sizes could not be identified easily, resulting in random and significant
62 measurement errors. In recent years, some researchers have applied the rare-earth-
63 elements (REE) tracing method to investigate the temporal and spatial distribution of rill erosion
64 (Zhang et al., 2009; Yan et al., 2009). This method successfully quantifies rill erosion but it is
65 time-consuming and requires specialized and expensive equipment.

66 In China, the study of rill erosion and sediment transport has concentrated
67 predominantly on the Loess Plateau. However, regions with purple soil have similar hydraulic
68 erosion. The purple-soil regions urgently require investigation, but related research is inadequate
69 and lacks systematic methodology. To date, researchers have adopted the use of artificial rainfall
70 simulations (Yan et al., 2010; Geng et al., 2010), but quantitative research on the process of rill
71 erosion in purple soil is still lacking.

72 In this study, we measured the amount of soil erosion along the rill length with
73 the volume-replacement method and calculated the sediment concentration along the length of
74 the rill. Our experimental flume was 12 m long so we could easily observe the sediment transport
75 from rill erosion even with a gentle slope and slow flow. We fit the experimental results to a
76 model describing the relationship between sediment concentration and rill length.

77 **2. The volume-replacement method for determining rill erosion**

78 Rill erosion is a critical factor underlying the high sediment concentration in water
79 flows on sloping land. In a model situation, sediment concentration increases rapidly at the inlet
80 of a rill and then the rate of increase subsequently slows. Once the sediment
81 concentration reaches a certain threshold, it stops increasing and rill sediment
82 concentration remains stable. At this point, the process in the rill switches from erosion to
83 sediment transport. If sediment concentration continues to increase and exceeds the sediment

84 transport capacity, sediment deposition occurs and can sometimes be observed in rills at a
85 particular distance down the rill. Following sediment deposition, the sediment concentration
86 decreases and new erosion can occur downstream. Therefore the rate of rill erosion and sediment
87 concentration estimated from the accumulated erosion amounts along the rill length may be
88 higher than the real values. Cycles of erosion and deposition appear randomly, with erosion and
89 deposition alternating both spatially and temporally.

90 Considering this, the basic assumptions of the volume-replacement method for
91 determining rill erosion are as follows:

- 92 1) The morphology of the eroded rill and the slope of the gully bed remain constant
93 during the measurement; that is, the influence of changing rill morphology on erosion
94 is ignored.
- 95 2) Rill water flow is also assumed to be stable over time, so erosion rates along the rill
96 length do not change with time.

97 With the above assumptions, the dynamic process underlying rill erosion is as follows: At
98 the rill inlet, the initial part of the rill flow, sediment concentration is zero. As erosion takes
99 place, sediment concentration increases, leading to a reduction in erosion along the rill length.
100 While there is no deposition, sediment concentration shows a net increase. When the sediment
101 particles begin to deposit, erosion alternates randomly with deposition. Sediment concentration
102 at the rill outlet is the maximum potential sediment concentration, as determined by the sediment
103 transport capacity of the flow. It similarly represents the average sediment concentration in time
104 and space of this section of the rill. Thus, the distribution of rill erosion is influenced mainly by
105 the initial section in which sediment content sharply increases (the major of net growth), and
106 sediment content along the rill is influenced mainly by the sediment export concentration.

107 Given the above, the process of rill erosion under different hydraulic conditions was
108 determined experimentally. Rill erosion was conducted under constant hydraulic conditions to
109 establish the changes in morphology along the rill. The total amount of water used for the rill
110 erosion was calculated from the flow rate and duration. The total soil erosion at different sites

111 along the rill was measured by the volume-replacement method. The average sediment
112 concentration (allowing for deposition as well as erosion) was calculated from the sediment
113 concentration in the collected runoff, and represents the maximum sediment concentration due to
114 rill erosion.

115 We measured the accumulated amount of erosion in each rill section to obtain the total amount of
116 erosion, then calculated the corresponding sediment concentration for each section. We could
117 thus obtain an integrated value for sediment concentration along the rill length, despite variations
118 in the rill morphology. Data values that were greater than the export sediment
119 concentration reflect the influence of sediment deposition and were replaced with the outlet
120 sediment concentration.

121 **3. Materials and Methods**

122 **3.1 Experimental materials and soil tank design**

123 Typical purple soil from the Southwest University experimental base for soil and water
124 conservation (106° 25' 45" E, 29° 49' 18" N) was collected for use in this study. The soil
125 contained 38.65% clay content (<0.005 mm), 35.74% silt content (0.005 – 0.05 mm), and 25.61%
126 sand content. The soil was air-dried before being crushed and passed through an 8 mm square
127 sieve. The experiment was conducted in the rainfall simulation hall at the Institute of Soil and
128 Water Conservation, Chinese Academy of Sciences and Ministry of Water Resources, Yangling,
129 Shanxi Province.

130 The laboratory flume measured 12 m × 3 m, and the central portion was divided into six
131 12 m × 0.1 m sections by upright PVC boards (Figure 1), to imitate well-defined rills and/or to
132 enable water flows to converge and form the required concentrated flow rate. Identical soil
133 materials were glued onto both sides of the PVC boards to imitate the roughness of the soil
134 surface to minimize boundary effects on rill erosion (Chen et al., 2013). The bottom 5 cm of the
135 flume was densely packed with clay soil to a bulk density of approximately 1500 kg m⁻³ to
136 imitate the plow pan layer. Above this layer, 20 cm of flume was packed with purple soil in

137 layers of about 5 cm to a bulk density of approximately 1300 kg m^{-3} to simulate the cultivated
138 layer. The soil near the flume walls was packed to be slightly higher than the soil near the middle
139 so that the water flow converged in the middle, which further minimized boundary effects. Prior
140 to the experimental runs, the prepared rills were saturated by running a rainfall simulator for 24 h
141 at an intensity of 60 mm/h to ensure that the water content was close to the field capacity.

142

143 **Figure 1 Experimental flume**

144

145 **3.2 Experimental design**

146 We simulated rill erosion at five different slopes (5° , 10° , 15° , 20° , 25°) and three
147 water flow rates (2 L/min, 4 L/min, 8 L/min, but see also section 2.3 below). The choice of flow
148 rate was determined by the critical rainfall intensities that produce rill erosion in sloping
149 croplands on purple soil, converted from rainfall to flow rates by artificial simulation of
150 rainfall intensity (Yan et al., 2011; Olson et al., 1989; Zhang et al., 2008; Lei et al., 2000).
151 Experimental water flow was controlled with an adjustable peristaltic pump. An additional,
152 specially designed, device was used at the rill flow inlet to accelerate the water flow to the
153 required velocity level. Approximately 0.2 m of gauze cloth was placed on the soil surface at the
154 rill inlet to protect the rill surface from being directly scoured by the water flow.

155 **3.3 Experimental methods**

156 All sediment samples were collected in a sampling bucket placed at the rill outlet. After a
157 the period of water scouring and rill erosion, the soil flume was adjusted to the horizontal. Plastic
158 film was twined in multiple layers to form eleven thin, waterproof, baffle plates the same width
159 as the rill. The baffles were inserted at 0.5 m, 1 m, 2 m, 3 m, 4 m, 5 m, 6 m, 7 m, 8 m, 10 m, and
160 12 m from the rill entrance, thus dividing the eroded rill into the following sections: 0 – 0.5
161 m, 0.5 – 1 m, 1 – 2 m, 2 – 3 m, 3 – 4 m, 4 – 5 m, 5 – 6 m, 6 – 7 m, 7 – 8 m, 8 – 10 m, and 10 – 12
162 m. The baffles were deep enough to prevent water from flowing between the rill sections.

163 Each section of rill was then filled with water and the soil erosion volume

164 was calculated by recording the volume of water in each rill section. Then the quality of soil
 165 erosion was calculated from the soil bulk. Unlike particulate matter such as soil, water fills the
 166 rill with no gaps. However, the impact of soil pores on the results can be excluded because the
 167 soil was pre-saturated. We obtained the values for rill erosion and sediment transport along the
 168 entire rill length from the cumulative values for each section.

169 Rill erosion proved to be low with a slope gradient of 5° and a flow rate of 8L/min, so the
 170 lower flow rates of 2 L/min and 4 L/min were not tested at this gradient. Similarly, we did not
 171 test the 2 L/min flow rate with a 10° slope because erosion was already very low at the 4 L/min
 172 rate. All other combinations of gradients and flows rates were tested, resulting in twelve
 173 different experimental conditions in total. Each condition was repeated three times, resulting in a
 174 total of 108 separate trials.

175 3.4 Calculation of sediment transport along the rill length

176 Sediment concentration refers to the dry mass of sediment per unit volume of water:

$$177 \quad S_{ci} = \frac{1000 \cdot M_{si}}{q \cdot \Delta t} \quad (1)$$

$$178 \quad M_{si} = \sum_{i=1}^{11} V_i \rho_b \quad (2)$$

179 In the formula, S_{ci} is the total sediment content at the end of the i th rill section (kg/m^3), M_{si} is the
 180 cumulative mass of eroded sediment at the end of the i th rill section (kg), q is the flow
 181 rate (L/min), Δt is the duration of each trial (min) (Zhao et al.,2014); V_i is the total volume of
 182 soil erosion in the i th rill section, as measured by the volume replacement method (m^3); ρ_b is the
 183 soil bulk density (kg/m^3). From equations (1) and (2), the sediment concentration can
 184 be calculated along the length of the rill, revealing the process of soil erosion along the rill length.

185 4 Results and Discussion

186 After observing the overall trends in the experimental data, we used the following model to
 187 fit the data and reveal how rill sediment concentration changes with rill length:

$$188 \quad C = A(1 - e^{-Bx}) \quad (3)$$

189 C represents the sediment concentration (kg/m^3); x represents the rill length
190 (m), A represents the maximum possible sediment concentration in the flow, (kg/m^3); B
191 represents the decay rate for sediment concentration with speed of rill length increasing ($1/\text{m}$).

192 Equation (3) represents a situation in which sediment concentration increases with
193 rill length, but the rate of increase decreases exponentially with distance along the rill, eventually
194 tending towards a stable sediment concentration, A . When B increases, the curve of the
195 exponential function becomes steeper for a particular value of A , meaning that the maximum
196 sediment concentration A is reached after a shorter distance along the rill. The experimental data
197 fits to the model in equation (3) are plotted in Figure 2, and demonstrate how purple-soil
198 sediment concentration varies along the rill length, for the different slopes and flow rates.

199

200

Figure 2 Sediment concentration as a function of rill length

201

202 The model parameters obtained under the different experimental conditions are listed in
203 Table 1. The coefficient of determination (R^2) was greater than 0.9 in each condition, indicating
204 that all fits to the model were very good. It can be seen from Figure 2 and Table 1 that the
205 tendency of purple-soil sediment concentration to increase with rill length was similar across
206 conditions. Under conditions of known slope gradient and flow rate, the data followed the model
207 closely: sediment concentration increased along the length of the rill but at a decreasing rate until
208 the sediment concentration tended towards a stable value, and the rate of increase tended to zero.

209 For slopes of the same gradient, the rate at which sediment concentration increased along
210 the rill length accelerated with increasing flow rates. The maximal sediment concentration
211 increased at higher flow rates, and the distance required to reach the maximal concentration
212 decreased. Similarly, for identical flow rates, the rate at which sediment concentration increased
213 along the rill length generally accelerated with steeper slopes. The maximal sediment
214 concentration increased for greater slopes, and the distance required to reach the maximal
215 concentration decreased. Overall, the influence of slope gradient was greater than the influence

216 of flow rate, and the tendency of sediment concentration to increase with rill length was more
217 obvious for changes in slope gradient than flow rate. When the underlying surface is the same,
218 the energy in the rill flow is defined by the net flow and current velocity, and the current velocity
219 is determined by the runoff depth and slope gradient. Runoff is the motive power behind soil
220 erosion on slopes. It scours, disperses, transports, and deposits the soil particles on the soil
221 surface, destroying the soil structure (Zhang et al., 2008). The frictional force between rill flow
222 and the soil surface influences the susceptibility to runoff scouring. In the context of our
223 experiment, slope gradient affects the soil stress distribution: when the slope was steeper, the
224 water flow dispersed and transported soil particles with greater speed and energy.

225

226 **Table 1 Sediment concentration model parameters obtained under different**
227 **experimental conditions**

228

229 Table 1 shows that, for identical slope gradients, parameter A increases with increasing flow
230 rates. A can be considered to be the maximal potential sediment concentration for purple-soil rill
231 flows. Our results therefore indicate that the maximal sediment concentration for purple-soil rill
232 flows increases with flow rate under conditions of constant slope gradient. Parameter
233 B represents the rate at which sediment concentration increases decay along the rill length. It can
234 be observed from Table 1 that B tended to increase with both slope gradient and flow rate,
235 indicating a faster rate of increase in purple-soil sediment concentration with steeper slopes and
236 greater flow rates. Similar results have been obtained in previous studies (Chen et al., 2014;
237 Chen et al., 2015).

238 **5. Conclusions**

239 In this study, we investigated the process of rill erosion along the rill length by using a 12 m
240 soil flume and the volume-replacement method. We used water to backfill the eroded rill
241 because of its mobility and the ease of volume measurement. We ensured that there were no
242 water leakages and so were able to quantitatively measure the process of rill erosion in purple

243 soil. The relationship between sediment concentration and rill length was obtained by fitting
244 the experimental data to a model with two free parameters. The results show that the sediment
245 concentration increases along the length of the rill, and tends towards a stable value. The rate at
246 which sediment concentration increases is highest at the rill entrance and then gradually
247 decreases along the rill length. With steeper slopes and faster flow rates, the increase in sediment
248 concentration is more obvious. These results may provide the basis for understanding the
249 mechanisms of rill erosion and may provide estimates for parameter values in future simulated
250 models of the erosion process in the purple soil.

251 **Acknowledgments**

252 This work was supported by the Foundation of Graduate Research and Innovation in
253 Chongqing under project CYS14054, and Construction Funds for Ecology Key Disciplines for
254 Project 211 Southwest University. We would like to thank Mr. Zhao J. and Mr. Wang C.B. for
255 providing guidance at the experimental facility.

256 **References**

- 257 Abrahams A.D., Parsons A.J., Hirsh P. J. et al., 1992. Field and Laboratory Studies of
258 Resistance to Interrill Overland Flow on Semi-arid Hillslopes, Southern Arizona.
259 London: UCL Press. 1-23.
- 260 Bhattarai R., Dutta D., Estimation of soil erosion and sediment yield using GIS at 295 catchment
261 scale, *Water Resour Manag.* 2007, 1635-1647
- 262 Cai Q.G., Zhu Y.D., Wang S.Y., Research on processes and factors of rill erosion. *Advances in*
263 *Water Science.* 15(1), 2004, 13-18
- 264 Casali J., Loizu J., Campo M.A., De Santisteban L.M. and Álvarez-Mozos J., Accuracy of
265 methods for field assessment of rill and ephemeral gully erosion, *Catena.* 67, 2006, 128–138
- 266 Chen J.J., Sun L.Y., Cai C.F. et al., Rill erosion on different soil slopes and their affecting factors
267 (in Chinese), *Acta Pedologica Sinica.* 50(2), 2013, 281-288
- 268 Chen X.Y., Zhao Y., Mo B., Mi H.X., An improved experimental method for simulating rill
269 erosion processes, *PloS One.* 9(6), 2014, 1-7

- 270 Chen X.Y., Zhao Y., Mi H.X., Mo B., Estimating rill erosion process from eroded morphology
271 in flume experiments by volume replacement method. *Catena*, doi:
272 10.1016/j.catena.2015.01.013. 2014.
- 273 Ellison W.D., Soil erosion studies. Part VI. Soil detachment by surface flow, *Agriculture*
274 *Engineering*. 28, 1947, 402-408
- 275 Foster G.R., 1982. Modeling the soil erosion process. Ch.5. In: Haan C T et al. *Hydrologic*
276 *Modeling of Small Watersheds*. ASAE, St. Joseph, MI.
- 277 Geng X.D., Zheng F.L., Liu L., Effect of rainfall intensity and slope gradient on the soil erosion
278 process on purple soil hill slopes, *Sediment Research*. 6, 2010, 48-53
- 279 Li Z.B., Zhu B.B., Li P., Advancement in study on soil erosion and water conservation, *Acta*
280 *Pedologica Sinica*. 45(5), 2008, 802-809
- 281 Lei T.W., Nearing M.A., Laboratory experiments of rill initiation and critical shear stress in
282 loose soil material (in Chinese), *Transactions of the CSAE*. 16(1), 2000, 26-30
- 283 Nearing M.A., Norton L.D., Bulgakov D.A., Hydraulics and erosion in eroding rills, *Water*
284 *Resources Research*. 33(4), 1997, 865-876
- 285 Olson K.R., Beavers A.H., Fan Z.G., Methods to estimate soil loss (in Chinese), *Scientific and*
286 *Technical Information of Soil and Water Conservation*. 2, 1989, 34-40
- 287 Xiao P.Q., Zheng F.L., Jia Y.Y., Loess hill slope erosion and sediment yield process using a dual
288 box system, *Science of Soil and Water Conservation*. 1(4), 2003, 10-15
- 289 Yuan Y., Wang Z.L., Liu J.N. et al., Experimental research on runoff-induced sediment discharge
290 processes of rill on loess hill slope, *Soil and Water Conservation*. 24(5), 2010, 88-91
- 291 Yan L.J., Yu X.X., Lei T.W. et al., Finite element model for calculating effects of slope flow
292 sediment transport capacity and soil erodibility on rill erosion process (in Chinese), *Acta*
293 *Pedologica Sinica*. 46(2), 2009, 192-200
- 294 Yan D.C., An W.B., Shi Z.L. et al., Critical slope length and control of rill occurrence on
295 cultivated land of purple soil in Sichuan Basin, *Research of Soil and Water Conservation*.
296 17(6), 2010, 1-4

- 297 Yan D.C., Wang Y.F., Wen A.B. et al., Configuration evolvement of rill development on purple
298 slope land (in Chinese), *Mountain Science*. 29(4), 2011, 469-473
- 299 Zhang Q.W., Lei T.W., Pan Y.H. et al., Dynamic sediment yield of rill erosion, *Transactions of*
300 *the CSAE*. 18(2), 2002, 32-35
- 301 Zhao H.B., Cao J.J., Yao W.Y. et al., Experimental study on process of sediment transport and
302 overland flow on the loess slope, *Research of Soil and Water Conservation*. 21(1), 2014, 90-
303 94
- 304 Zheng F.L., A research on method of measuring rill erosion amount, *Bull. Soil Water*
305 *Conserv.* 9 (4), 1989, 41-49.
- 306 Zhang Q.W., Lei T.W., Zhao J., Study of detachment rate in rills with the REE tracing method
307 (in Chinese), *Acta Pedologica Sinica*. 42(1), 2009, 163-166.
- 308 Zhang Q.W., Lei T.W., Zhao J., Estimation of the detachment rate in eroding rills in flume
309 experiments using an REE tracing method, *Geoderma*. 147, 2008, 8-15
- 310 Zhao Y., Chen X.Y., Mi H.X. et al., A volumetric method based study on distribution of erosion
311 along rills on loess slope, *Acta Pedologica Sinica*. 51(6), 2014, 1234-1241
- 312

Figure 1(on next page)

Experimental flume

Fig1- Experimental flume

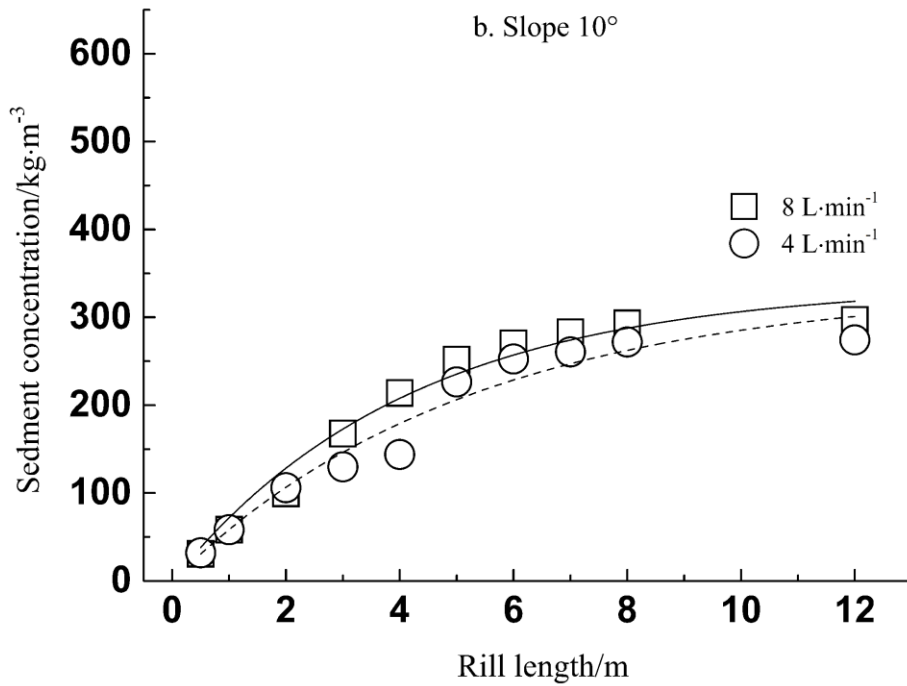
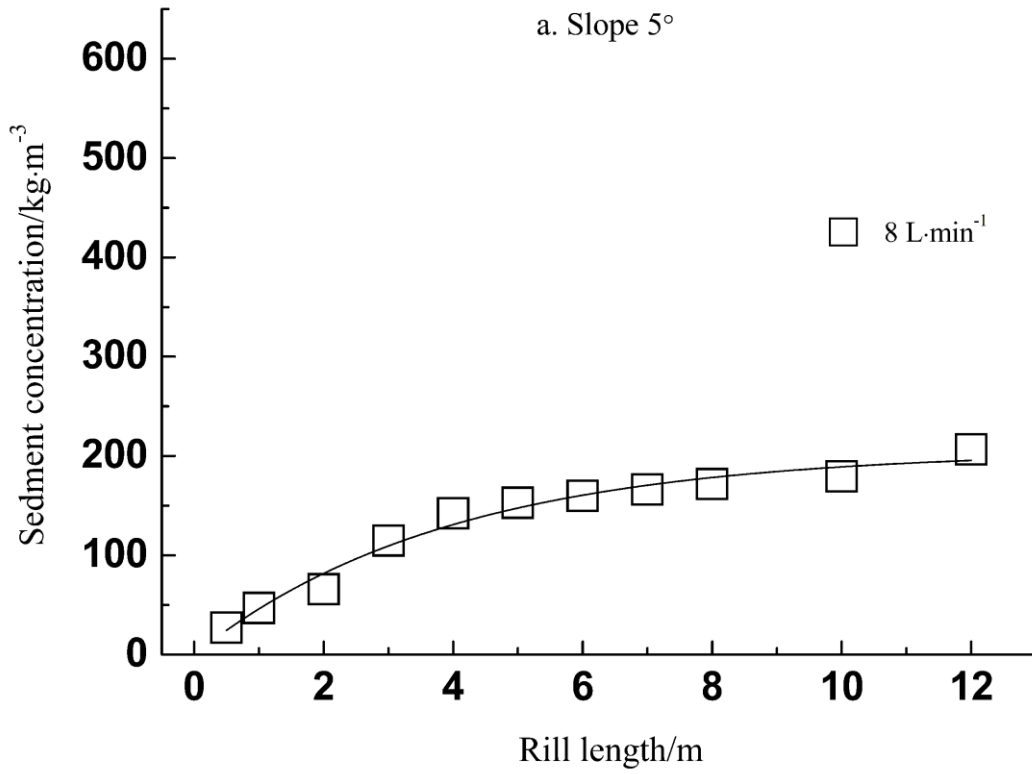


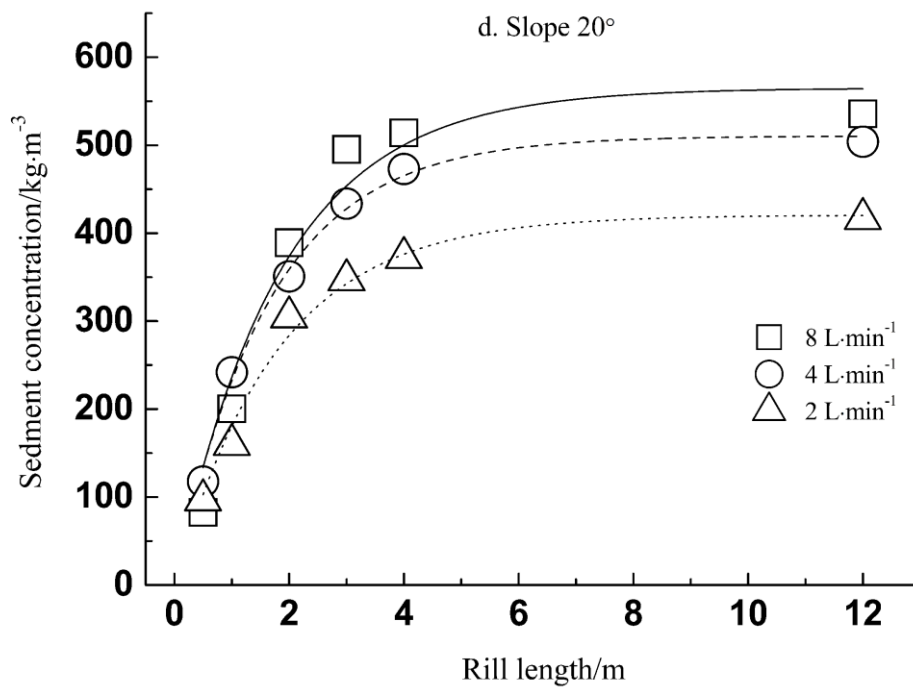
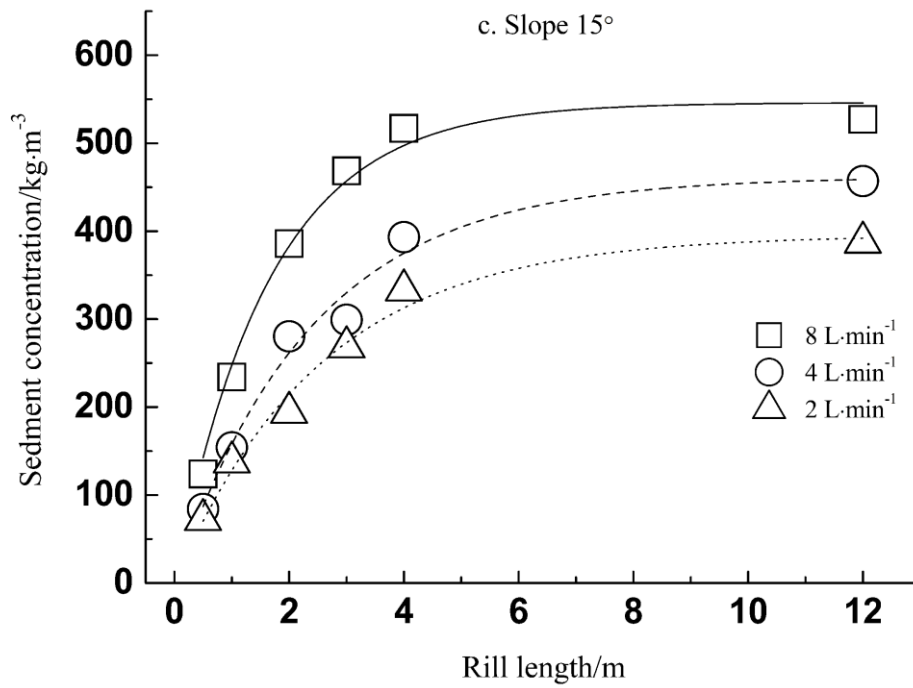
Figure 1 Experimental flume

Figure 2 (on next page)

Sediment concentration as function of rill length

Fig 2- Sediment concentration as function of rill length





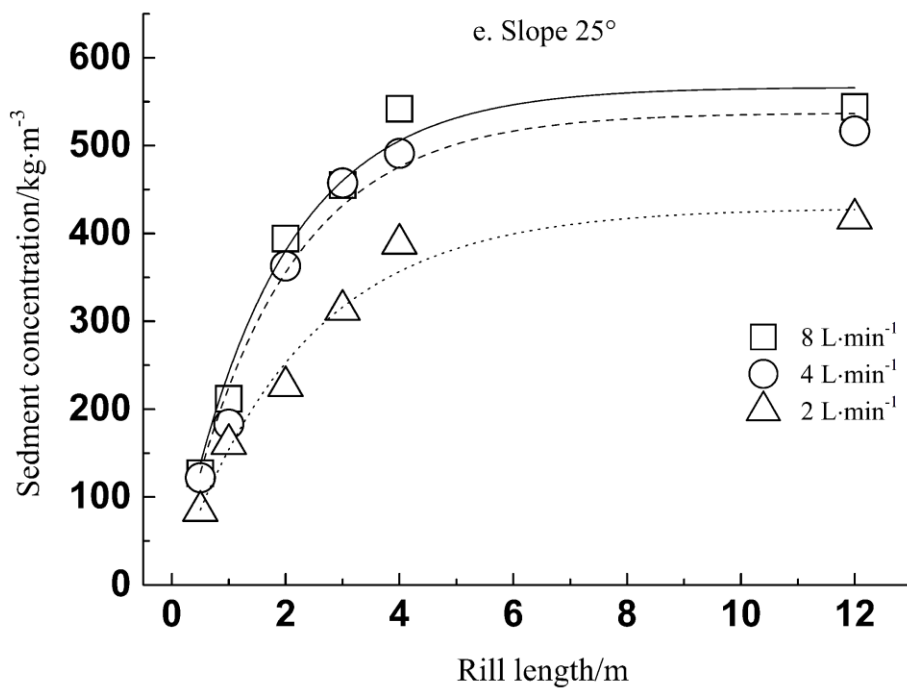


Figure 2 Sediment concentration as a function of rill length

Table 1 (on next page)

Sediment concentration model parameters obtained under different experimental conditions

Tab-1 Sediment concentration model parameters obtained under different experimental conditions

Table 1 Sediment concentration model parameters obtained under different experimental conditions

<i>Slope gradient</i> /(°)	<i>Flow rate</i> /(L·min ⁻¹)	<i>Regression parameters</i>		<i>Coefficient of determination</i>
		<i>A</i>	<i>B</i>	<i>R</i> ²
5	8	206.56	0.25	0.98
10	4	274.39	0.28	0.93
	8	296.88	0.31	0.96
15	2	387.31	0.41	0.99
	4	456.93	0.43	0.99
	8	532.97	0.64	0.99
20	2	395.84	0.64	0.98
	4	476.80	0.70	0.99
	8	548.56	0.57	0.96
25	2	451.71	0.41	0.99
	4	499.22	0.62	0.96
	8	595.11	0.51	0.99